

---

# *Ab initio* calculations on the Al<sub>2</sub>O<sub>3</sub>(0001) surface

---

Iskander Batyrev, Ali Alavi and Michael W. Finnis\*

*Atomistic Simulation Group, School of Mathematics and Physics, The Queen's University of Belfast, Belfast, UK BT7 1NN*

*Received 26th April 1999*

We calculate using a density functional pseudopotential method the atomic and electronic structure of the (0001) surface of  $\alpha$ -alumina (Al<sub>2</sub>O<sub>3</sub>). The material is studied in the form of a slab with periodic boundary conditions, containing up to eight layers of the stoichiometric Al<sub>2</sub>O<sub>3</sub> units. Five different terminations of the surface are calculated, representing different surface excesses of oxygen, and their free energies are estimated as a function of oxygen partial pressure. Internal relaxations of the atomic positions are obtained. The aluminium terminated surface, which is stoichiometric, has the lowest surface energy for a wide range of oxygen pressures.

---

## 1. Introduction

The (0001) surface of  $\alpha$ -Al<sub>2</sub>O<sub>3</sub> (corundum or sapphire) has been studied experimentally and theoretically for many years since it is a widely used substrate for many kinds of thin films and an archetypal wide band-gap ionic oxide. This surface terminates a layered structure, in which each oxygen plane in the bulk has an associated aluminium plane at a distance 0.838 Å above and below it, forming a stoichiometric triple layer. The most convenient unit cell is a rhombohedral prism comprising six such (0001) oxygen planes separated by the associated pairs of aluminium planes. The cell contains just one atom in each Al plane and three atoms in each O plane. In the bulk structure the oxygen planes are separated by 2.166 Å and form a hexagonal lattice with ABABAB . . . stacking. Their positions are slightly laterally distorted from ideal hexagonal sites. The Al atoms occupy two-thirds of the octahedral holes in the oxygen sublattice, at positions which alternate above and below the centres of these holes. The unoccupied octahedral holes are themselves stacked on a face-centred cubic lattice, abcabc . . . A C<sub>3v</sub> symmetry axis passes through each Al atom and through the centres of the unoccupied octahedral sites. Fig. 1 shows an elevation of the structure.

Only recently, with the advent of grazing incidence X-ray diffraction, has it become possible to compare structural predictions for the (0001) surface directly with experiment. Renaud has published a comprehensive review of the experimental and theoretical results.<sup>1</sup> The normally observed structure is (1 × 1), for which one can postulate three possible bulk terminations: single Al, double Al or O. The observed surface is believed to be terminated by a single Al plane, as in Fig. 1 in which this plane is labelled Al1. This termination is stoichiometric, that is, it exhibits no surface excess of Al or O. The top layers relax strongly; best estimates of the interlayer relaxations of the top four layers from experiment<sup>2</sup> are -51%, 16%, -29% and +20%.

Manassidis *et al.*<sup>3</sup> were the first to use density functional theory (DFT) within the local density approximation (LDA) for exchange and correlation, to calculate the energy and relaxation of this surface. They used a pseudopotential approach and modelled the surface with a slab containing

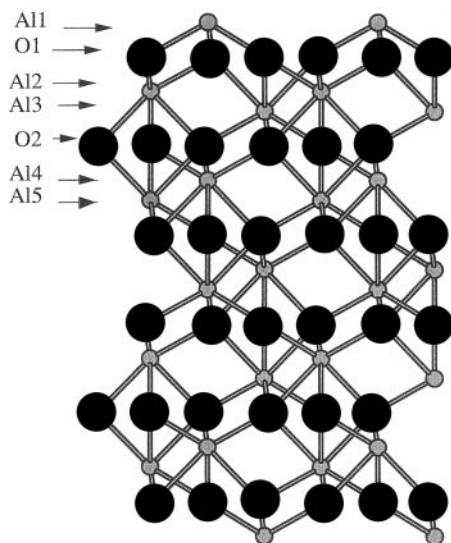


**Fig. 1** View of the corundum lattice terminated at the (0001) surface by the Al plane labelled Al1. This is the stoichiometric termination ( $\Gamma_{\text{O}} = 0$ ) and the main one observed experimentally.

three layers of oxygen. The most striking feature of the surface is the large inward relaxation of the surface Al plane, which in this calculation reduces the first interplanar spacing by 85%. Their results were later confirmed with a similar calculation by Kruse *et al.*<sup>4</sup> A recent DFT calculation by Verdozzi and co-workers<sup>5</sup> again confirmed the large surface relaxation; they used slabs containing up to 18 layers of oxygen, eliminating any uncertainty as to the effect of finite slab thickness. Their use of a thicker slab also enabled them to predict the interlayer spacings of deeper layers. For the first four layers they found relaxations of  $-87\%$ ,  $+3\%$ ,  $-42\%$ ,  $+19\%$ .

Puchin *et al.*<sup>6</sup> have also calculated the atomic and electronic structure of the stoichiometric, Al-terminated surface modelled as a slab containing 3 layers of oxygen. They used the Hartree–Fock (HF) method (embodied in the CRYSTAL code) with an 85-11G/8-411G basis set for each atom. The surface Al layer was found to relax inwards by 68%, somewhat less than the DFT calculations, (the difference being 0.016 nm), but significantly more than the previous HF results (48%) using a smaller basis.<sup>7,8</sup> Puchin *et al.* went on to calculate theoretical UV photoelectron spectra (UPS) and metastable impact electron spectra (MIES), and compared them with experiment, concluding that the model gave a good description of the surface resolved density of states (DOS) in the valence band, and even that the relaxation was more consistent with these experimental data than the somewhat larger DFT relaxation.

Calculations of the atomic and electronic structure of the (0001) surface have been made with a non-self-consistent tight-binding model by Godin and LaFemina.<sup>9</sup> They also reported a very large ( $>90\%$ ) relaxation of the surface Al layer, which they attributed to the formation of almost planar  $sp^2$  bonds between the surface Al and the O triangle on which it sits. However, this large relaxation was also found in the earliest studies with classical ionic interatomic potentials,<sup>10</sup> which of course have no representation of chemical bonding, whether  $sp^2$  or  $sp^3$ .

We note the above discrepancy between the interpretations of the large inward relaxation of the surface Al layer. The argument in terms of bond hybridisation we find less persuasive than the simple electrostatic argument; because (a) ultimately the driving force for any relaxation or reconstruction is the classical electrostatic force on the relaxing ion from the self-consistent charge density (the Hellmann–Feynman theorem) and (b) in the first-principles calculations there is no sign of  $sp^2$  bonding in the charge density distribution, which looks very ionic. There are other seemingly contradictory statements and observations concerning this surface which are worth discussing here. It was noted for example by Godin and LaFemina<sup>9</sup> that the surface Al–O bond length is conserved (to within 10%) as the Al relaxes inwards, which is effected by an associated expansion of the O triangle. Their tight binding model showed this effect, and it is also apparent

from the X-ray data referred to above, from which the Al–O bond length is only 4.5% ( $\pm 2.5\%$ ) shorter than the bulk nearest neighbour value. However, it is not the case, as Godin and LaFemina speculated, that the outward lateral relaxation of the O triangle is a *necessary* condition for the large inward relaxation of the Al (by analogy with semiconductor surfaces and their bond-length conserving reconstructions), because the earlier first-principles calculations of large Al relaxation<sup>3,4</sup> did not allow lateral relaxations at all. In the present paper, we report first-principles calculations for this surface including full relaxation of all atomic co-ordinates in the unit cell, and discuss the pattern of relaxation in some detail. The nature of the electrostatic driving force for the Al relaxation has also been described as reducing the electrostatic dipole of the first two atomic layers, in the manner of the attraction between the plates of a capacitor. This seems a satisfactory explanation, as long as one bears in mind that the first *three* atomic layers (Al–O–Al . . .) of the structure form an electrically neutral object in the sense of the ionic model.

Another argument which has sometimes been aired, is that only the single Al terminated surface should be stable because an alternative ( $1 \times 1$ ) surface, such as the one terminated by an O plane, would be charged and therefore have an infinite surface energy. This is clearly only the case within a purely ionic model in which all ions carry their bulk formal charges. However, it is a poor basis for discussing the present surface, especially since it is now known experimentally that there are other rather stable terminations of it. In particular, on heating in UHV, this surface undergoes a series of reconstructions culminating in a  $(\sqrt{31} \times \sqrt{31})R \pm 9^\circ$  structure at around 1350 °C; *R* indicates that the reconstructed layer is rotated with respect to the substrate. This structure has now been characterised<sup>11</sup> and is believed to comprise domains of nearly two Al(111) layers, formed by losing the first two layers of oxygen from the stoichiometric ( $1 \times 1$ ) surface discussed above.

A major aim of the present paper is to describe how the relative energetics of surfaces of different stoichiometry can be calculated theoretically. There is one independent variable needed to compare the surface energies of surfaces of differing stoichiometry (or surface excess of one component), and that is most usefully taken to be the partial pressure of oxygen, since this is what is most directly under the control of the experimentalist. We formulate the theory in Section 3 with this in mind. First, in the following section, we describe briefly our method of calculation of total energies, which provide input to the theory. While we have insufficient computer resources to make calculations for the  $(\sqrt{31} \times \sqrt{31})R \pm 9^\circ$  surface, we shall illustrate how this could be done, in principle, by comparing the energetics of five alternative ( $1 \times 1$ ) surfaces of differing stoichiometry. This will also show that previous arguments based on classical electrostatics for the stability of the stoichiometric, Al-terminated surface are of doubtful validity. We find, for example, that the O-terminated surface could in theory be stabilised by a moderately high pressure of oxygen. Our results are described in Section 4 and we conclude in Section 5.

## 2. Method of calculation

We base our total energy calculations on a supercell with periodic boundary conditions, which enables us to use a basis of plane waves. The supercell has the form of a rhombohedral prism, and in the stoichiometric slab it contains 30 atoms. This slab is exactly the thickness of one bulk unit cell of the corundum structure.

Our surface calculations are made on slabs of this kind repeated periodically in the *z* direction, with a vacuum space of thickness about equal to that of the slab. This is adequate to isolate the surfaces. The stoichiometric slab has two equivalent surfaces, which are terminated by an Al plane, as in Fig. 1, in which our labelling of the atoms is shown. This termination *defines* the stoichiometric surface, because the slab as a whole is stoichiometric and has two equivalent surfaces. We note as an aside that surfaces which are not stoichiometric are sometimes called polar. Besides the stoichiometric surface, we have studied four non-stoichiometric surfaces, two with an oxygen excess and two with an aluminium excess. By stripping off the surface plane of Al we obtain a surface which is O terminated, with an O excess of +1.5 atoms per unit surface cell, or an Al excess of  $-1$  atoms per unit surface cell (see eqn. (5) below). We can then proceed to remove the three surface O atoms one at a time, giving three more surfaces with O excesses of 0.5,  $-0.5$  and  $-1.5$ , respectively. The final surface is terminated by two layers of Al. In the actual calculations we ensure that the surfaces on each side of our slab are equivalent (to avoid a dipole moment in

the supercell). Thus we actually add a seventh layer of oxygen to create the O-terminated surfaces and remove a layer of oxygen to create the most Al-rich surfaces.

The total energy of the contents of a supercell is minimised with respect to the electronic co-ordinates (the coefficients of each plane wave in each occupied wave function) and the atomic co-ordinates, as described in previous work.<sup>12,13</sup> The ionic potentials are represented by pseudo-potentials of the Troullier–Martens form.<sup>14</sup> All the calculations were made with two k-points in the irreducible (120°) wedge of the Brillouin zone, and with a plane-wave cut-off of 40 Ry. Convergence tests were reported previously.<sup>15</sup>

In order to obtain information about the charge redistribution at these surfaces we calculate the Mulliken populations. These are defined by the formalism of Mayer.<sup>16</sup> In our case we use the pseudo-orbitals  $|\varphi_{ia}\rangle$  as a basis for projection, which includes O 2s, O 2p, Al 3s and Al 3p components (labelled  $\alpha$ ) on each site (labelled  $i$ ). The “spillage” of each occupied orbital  $\psi$ , defined as  $1 - \sum_{ia} |\langle \psi | \varphi_{ia} \rangle|^2$ , with this atomic-like basis is less than 1.5%.

### 3. Surface energy and oxygen partial pressure

We have chosen here to discuss the regime we think is more likely to be encountered in practice, in which the  $\text{Al}_2\text{O}_3$  surface is in equilibrium with Al and O in the vapour phase, rather than the regime in which it is in equilibrium with Al in the solid or liquid phases. Since there are two components, the temperature  $T$  and pressure  $P$  are two independent variables which can be used to specify the state of the system. To be of use in experimental situations our final formula for the surface energy will be couched in terms of the chemical potential ( $\mu_{\text{O}}$ ) or partial pressure ( $p_{\text{O}_2}$ ) of oxygen rather than the total pressure  $P$ .

We adopt the thermodynamic definition of surface excesses due to Gibbs, most clearly described by Cahn.<sup>17</sup> For future application to other oxides, we derive here the general formula appropriate to an oxide of metal M with the stoichiometric composition  $\text{M}_m\text{O}_n$ . The surface energy  $\gamma$  in this case is given by:

$$\gamma(T, P) \cdot A = G_{\text{slab}}(T, P) - N_{\text{M}} \mu_{\text{M}}^{\text{v}}(T, P) - N_{\text{O}} \mu_{\text{O}}(T, P) \quad (1)$$

in which  $A$  is the area of the surface within the supercell, counting both surfaces of the slab.  $G_{\text{slab}}$  is the Gibbs energy of the contents of the supercell, and  $N_{\text{M}}$  and  $N_{\text{O}}$  are the total number of atoms of metal and oxygen, respectively, within the supercell.  $\mu_{\text{M}}^{\text{v}}$  is the chemical potential of the metal, and we use the superscript v to emphasise that at the temperature of interest the metal is in the vapour phase. If this were not the case we would be dealing with an interface of the solid or liquid metal with its oxide, and this would require a different treatment. In a supercell of a few tens of atoms, such as we use for *ab initio* calculations, all the atoms can be assumed to be in the solid phase and approximately half of the supercell is a true vacuum. No serious error is made in eqn. (1) by omitting the statistical occurrence within the supercell of atoms in the vapour phase. Likewise, no significant error is made by not explicitly including the presence of point defects within the solid part of the supercell. It is more problematic that we are ignoring the surface terminations involving a statistical distribution of defects, as in a partial layer of adsorbed oxygen.

The chemical potential of oxygen is given in terms of its partial pressure  $p_{\text{O}_2}$  by the ideal gas expression:

$$\mu_{\text{O}} = \mu_{\text{O}}^{\circ} + \frac{1}{2}kT \ln p_{\text{O}_2} \quad (2)$$

in which we use superscript  $\circ$  to denote the standard state (STP), and the pressure is in units of atmospheres. We choose to define the chemical potentials per atom rather than per mole. In order to relate  $\gamma(T, P)$  to  $p_{\text{O}_2}$  we wish to insert eqn. (2) into eqn. (1). Two problems arise at this point. First, in *ab initio* calculations the zero of free energy is the energy of separated free ions and electrons at rest; this is not the usual convention, which is the free energy of the elements at STP. With the latter convention,  $\mu_{\text{O}}^{\circ} = 0$ , but the convention of our calculations means that if we use eqn. (2) to evaluate eqn. (1) we still have to know the value of  $\mu_{\text{O}}^{\circ}$ . Secondly, the free energy of oxygen in the vapour phase is a quantity we wish to avoid calculating explicitly. Because of the paramagnetic nature of oxygen, even the energy of a molecule at rest would require a more accurate treatment than the local density approximation for exchange and correlation, which is

adequate for solid phases. We can deal with both these problems by making use of experimental thermodynamic data, as follows.

First, we can use the equilibrium of the two phases to eliminate the chemical potential of the metal vapour in favour of the Gibbs energy per formula unit of the metal oxide,  $G_{\text{MO}}$ :

$$G_{\text{MO}} = m\mu_{\text{M}}^{\text{v}} + n\mu_{\text{O}}. \quad (3)$$

Inserting eqn. (3) into eqn. (1) gives:

$$\gamma(T, P) = \frac{1}{A} (G_{\text{slab}}(T, P) - \frac{1}{m} N_{\text{M}} G_{\text{MO}}(T, P)) - \Gamma_{\text{O}} \mu_{\text{O}}(T, P) \quad (4)$$

in which we have introduced the surface excess of oxygen with respect to the metal, defined by<sup>17,18</sup>

$$\Gamma_{\text{O}} = \frac{1}{A} \left( N_{\text{O}} - \frac{n}{m} N_{\text{M}} \right). \quad (5)$$

Next we use the definition of the standard Gibbs energy of formation to obtain the oxygen chemical potential in its standard state:

$$G_{\text{MO}}^{\circ} = m\mu_{\text{M}}^{\circ} + n\mu_{\text{O}}^{\circ} + \Delta G^{\circ}. \quad (6)$$

Combining eqn. (6) with eqn. (4) and (2) gives:

$$\begin{aligned} \gamma(T, P) = & \frac{1}{A} \left( G_{\text{slab}}(T, P) - \frac{1}{m} N_{\text{M}} G_{\text{MO}}(T, P) \right) \\ & - \Gamma_{\text{O}} \left( \frac{1}{n} G_{\text{MO}}^{\circ} - \frac{m}{n} \mu_{\text{M}}^{\circ} - \frac{1}{n} \Delta G^{\circ} \right) - \Gamma_{\text{O}} \frac{1}{2} kT \ln p_{\text{O}_2}. \end{aligned} \quad (7)$$

Eqn. (7) is the result we were seeking. The first term is calculated at 0 K, and we omit its temperature dependence. In principle, one could perform a molecular dynamics simulation and, by means of thermodynamic integration from 0 K to T, obtain the temperature dependence of this term. Alternatively, at temperatures not too close to the melting point, it could be estimated from a calculation of the phonon frequencies of the slab and of a comparison piece of bulk material, using the quasiharmonic approximation. The accuracy of both approaches is limited by the sample size but we feel that either would be reasonable since the result is an integrated quantity localised near the surface. The first term is also where a large cancellation takes place between the difference of two energies which scale with the number of atoms leaving a superficial quantity. It is therefore advantageous to use an identical cell and k-point mesh for the slab and bulk terms in it.

The quantities  $G_{\text{MO}}^{\circ}$  and  $\mu_{\text{M}}^{\circ}$  entering the second term are well described by 0 K quantities, which we calculate. It can be verified that correcting them to STP has a negligible effect on the surface energy. Finally  $\Delta G^{\circ}$  is taken from experimental thermodynamic data. This leaves the  $p_{\text{O}_2}$  term as the one that describes the important variation of  $\gamma$  with temperature and oxygen partial pressure. Notice that in the case of a stoichiometric termination, only the first term is non-zero, and this describes the elementary case in which the energy of bulk phase is subtracted from the energy of a slab containing exactly the same number of molecules.

The minimum physically meaningful value of  $p_{\text{O}_2}$ , which we denote  $p_{\text{O}_2}^{\text{min}}$ , is set by the condition that at  $p_{\text{O}_2} \leq p_{\text{O}_2}^{\text{min}}$  the oxide would spontaneously decompose into metal and oxygen. This would be the case if

$$\mu_{\text{M}}^{\text{c}}(T, P) \leq \mu_{\text{M}}^{\text{v}}(T, P) \quad (8)$$

where  $\mu_{\text{M}}^{\text{c}}(T, P)$  denotes the chemical potential of the metal in its condensed phase. The result in terms of  $p_{\text{O}_2}$  is fairly well known, but we briefly rederive it here for completeness. Substituting eqns. (3) and (6) into eqn. (8) and rearranging the inequality gives:

$$\mu_{\text{O}} - \mu_{\text{O}}^{\circ} \leq \frac{1}{n} \Delta G^{\circ} + \frac{1}{n} (G_{\text{AO}}(T, P) - G_{\text{AO}}^{\circ}) - \frac{m}{n} (\mu_{\text{M}}^{\text{c}}(T, P) - \mu_{\text{M}}^{\circ}). \quad (9)$$

From the specific heat data of the solids we know that the second and third terms are about two orders of magnitude smaller than the first in alumina, and we expect them to be negligible in general. Hence we obtain the relation:

$$\ln p_{\text{O}_2}^{\text{min}} = \frac{2}{nkT} \Delta G^\circ. \quad (10)$$

It is worth noting that the above formulae could be applied directly to calculate the energy of oxide/metal interfaces. All that is required is to subtract from eqn. (7) the energy of the same amount of bulk phase of the metal with which the oxide is in contact. In this case  $G_{\text{slab}}$  would refer to a supercell containing a slab of oxide in contact with metal and there would be no vacuum space.

#### Note on nomenclature for surface excess

In the remainder of this paper we shall characterise the surface terminations by the natural unit of oxygen surface excess  $\Gamma_{\text{O}}$ , which is atoms per surface unit cell rather than atoms per unit area of the slab. This is equivalent to setting  $A = 2$  in the above equations (since there are two surfaces in the supercell). A simple algorithm to determine the surface excess for a given surface which does not rely on having equivalent surfaces on a slab is given by Finnis.<sup>18</sup>

## 4. Results and discussion

### 4.1. Surface relaxation

The interlayer relaxations are accompanied by  $x$ - $y$  (in-plane) relaxations of the three O atoms per plane in each unit cell. The manner of these in-plane relaxations is illustrated in Fig. 2. The Al atoms do not relax laterally but remain aligned along  $z$  to preserve the threefold axes. Since the three O atoms above an empty octahedral site in each plane are symmetry related and lie at the corners of an equilateral triangle, their lateral relaxation can be characterised by two parameters,

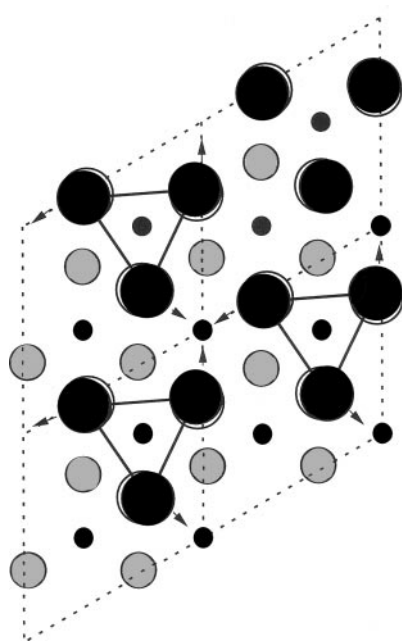


**Fig. 2** Plan view of the (0001) surface illustrated in Fig. 1 ( $\Gamma_{\text{O}} = 0$ ), showing the lateral relaxations within the topmost O plane. The relaxed positions are shaded black. The rotation and expansion of the triangle below Al is indicated.

which we take to be the rotation of the triangle and the linear expansion or bond length change of the triangle. This is the triangle on which the surface Al atoms labelled Al1 in Fig. 1 are centred. The magnitudes of the relaxations for three surfaces are reported in Table 1.

We find for the  $\Gamma_{\text{O}} = 0$  surface, the only one for which a comparison with experiment is possible, qualitative agreement between calculations and experimental measurements. The most marked effect is the well known strong inward relaxation of Al1, which we calculate to be 77%, and which as in the previous published calculations of this quantity, is significantly larger than the experimental value of 51%. The accompanying expansion and rotation of the O1 triangle centred on an axis through Al1 are calculated to be 3.2% and  $3.05^\circ$ , compared to the experimental values of 4.2% and  $6.7^\circ$ . These are quantities for which predictions have not previously been compared directly to experiment. We believe that Al1 as it relaxes is squeezing the O1 triangle open. This triangle rotates so as to allow the O1 atoms to approach Al2 rather than to move towards other O1 atoms in the same plane. There are three symmetry-equivalent O1 atoms which thereby form a more constricting triangle about each Al2 atom, so the interplanar O1–Al2 distance, not surprisingly, increases. This is our interpretation of the 10.6% calculated O1–Al2 interplanar relaxation, which is 16% experimentally. Unfortunately previous calculations give a much smaller or even negative value for this parameter. We tend to discount the tight-binding results in this comparison, because they showed the opposite sign for the third layer (Al2–Al3) relaxation compared to ours and experiment. Nevertheless, there remains a significant discrepancy between theory and experiment and even between the first-principles theories for which we have no satisfactory explanation.

The calculations predict a similar rotation–expansion of the O1 triangle for the  $\Gamma_{\text{O}} = 1.5$  (oxygen terminated) surface. In this case, the topmost interlayer spacing contracts by 14.6%, and these relaxations can be consistently explained by the electrostatic pull of the Al2 ions.

## 4.2. Mulliken charges

The total charges on each ion calculated from the Mulliken population analysis are shown in Table 2. Caution is needed in interpreting these data for two reasons. First, because the local basis is not complete the Mulliken charges do not exactly balance the ionic charges. For example, each formula unit carries an ionic charge of  $2 \times 3 + 3 \times 6 = 24$ . A spillage of 1% therefore corresponds

**Table 1** Calculated relaxations of the O-terminated ( $\Gamma_{\text{O}}=1.5$ ), Al-terminated ( $\Gamma_{\text{O}}=0$ ) and double Al-terminated ( $\Gamma_{\text{O}} = -1.5$ ) surfaces<sup>a</sup>

	$\Gamma_{\text{O}}$			
	1.5	0	0(exp)	-1.5
O-Rotation	4.12	3.05	6.7	0.60
O-Expansion	4.30	3.20	4.2	0.62
Al1–O1	—	-77.0 (-70.3)	-51	—
O1–Al2	-14.6	+10.6 (+13.9)	16	—
Al2–Al3	+6.8	-34.3 (-38.3)	-29	+13.9
Al3–O2	+12.1	+18.5 (+22.5)	20	+7.9
O2–Al4	-3.6	+1.0 (+9.5)		+7.7
Al4–O5	-14.9	-1.9 (-4.1)		+1.0

<sup>a</sup> The supercells contained 33, 30 and 27 atoms, respectively. Values in parentheses for  $\Gamma_{\text{O}} = 0$  were calculated for a thinner slab of only 20 atoms, and are shown in order to give an indication of finite size effects. The third column contains experimental results.<sup>2</sup> The first row shows the rotation of the topmost O triangle, which is measured in degrees, all other relaxations are given in percentages of bulk distances: the second row gives the O–O expansion of the topmost O triangle and subsequent rows give interplanar relaxations. The topmost O triangle contains the atoms labelled O1 except for the double Al termination, for which the topmost O atoms are O2.

**Table 2** Mulliken + ionic charges for atoms near the surface<sup>a</sup>

	$\Gamma_{\text{O}}$				
	+1.5	+0.5	0	-0.5	-1.5
Al1	—	—	1.72	—	—
O1	-0.58	-0.76	-1.03	-0.93	—
Al2	1.69	1.65	1.54	1.20	0.75
Al3	1.66	1.61	1.57	1.43	0.88
O2	-0.99	-0.99	-0.99	-1.03	-1.01
Al bulk	1.57	1.57	1.57	1.57	1.57
O bulk	-1.00	-1.00	-1.00	-1.00	-1.00

<sup>a</sup> The columns label the five surfaces by their surface excess of O in atoms per unit surface cell. The notation for atomic planes is as in Fig. 1.

to 0.24 “missing” electrons per formula unit. We have not sought to allocate these missing electrons in any way, which would certainly be arbitrary. Secondly, because the local basis itself is not unique, the charge transfers calculated are not unique and a different choice of basis would give different results. However, the *trends* in charge transfer can be interpreted in a meaningful way, which will not be different if the charges themselves are redefined by a different choice of local orbitals. With these caveats in mind we comment on the results in Table 2.

First, considering the  $\Gamma_{\text{O}} = 0$  surface, the surface ionic charges are similar to the bulk but the ionicity is slightly enhanced. The charge on Al1, for example, is 1.72 compared to 1.57 in the bulk, an extra charge which is mostly drawn from Al2. There is certainly no sign of increased covalence, which one might have associated with the large relaxation of Al1.

Secondly, on the O terminated surface ( $\Gamma_{\text{O}} = 1.5$ ) the surface O is carrying 0.58 electrons compared to 1.0 in the bulk. As the oxygen excess is reduced to zero the number increases from 0.58 to 1.03, slightly exceeding the bulk value. Correspondingly, as the oxygen excess decreases and becomes negative the topmost Al tends to carry less charge. In the most Al-rich case ( $\Gamma_{\text{O}} = -1.5$ ) the bulk charge on Al of 1.57 is roughly shared between the two surface layers of Al (0.75 and 0.88). These large variations in surface charge highlight the well known difficulty of using an ionic model in all but stoichiometric situations.

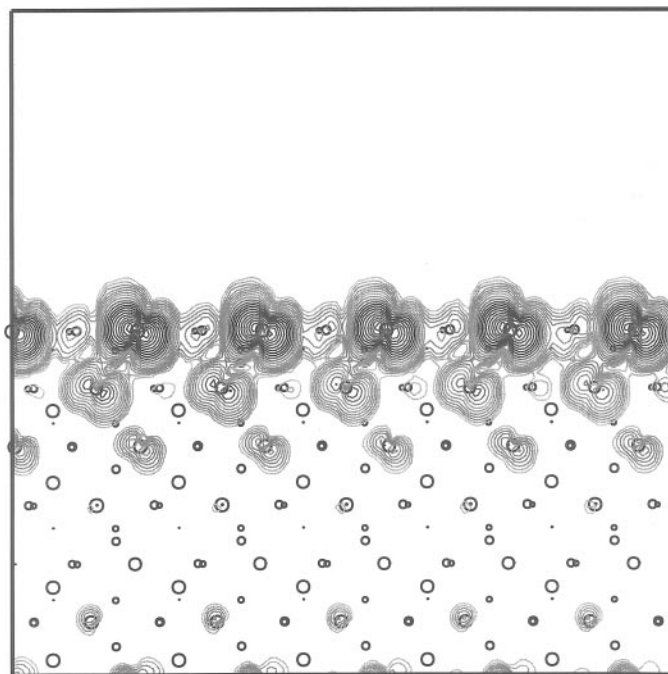
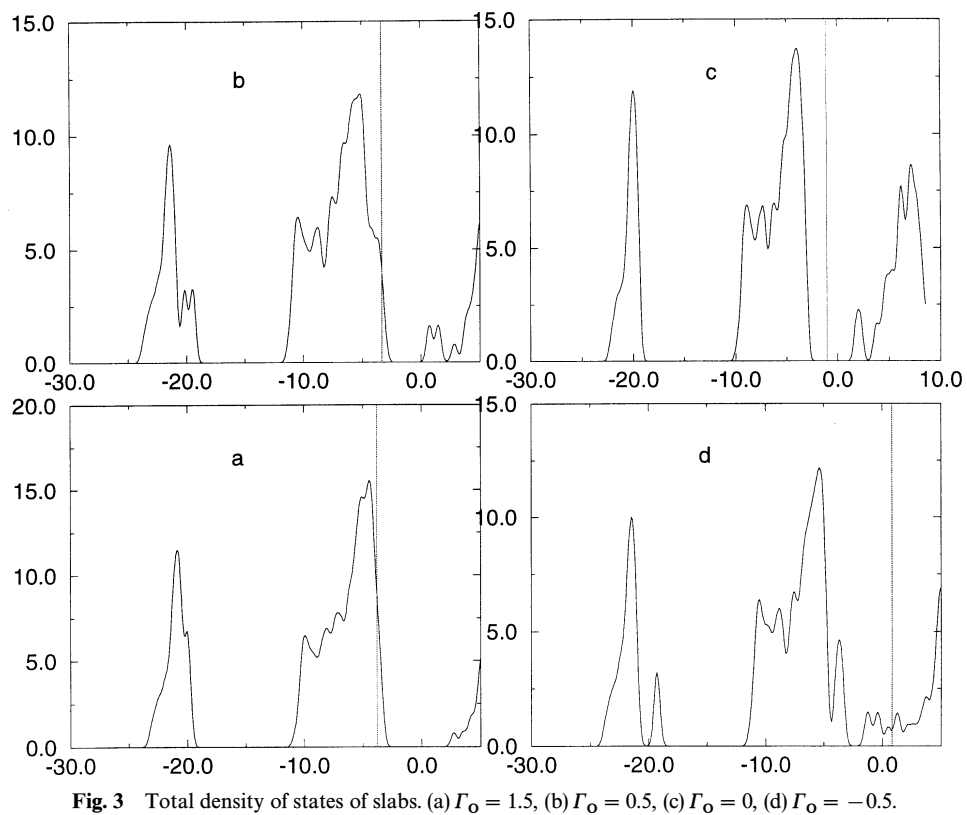
#### 4.3. Densities of states

The stoichiometric surface is known from calculations to be insulating with a large band gap like the bulk material, however in the non-stoichiometric surfaces two kinds of surface metallisation can be expected. For Al-rich surfaces the charge on Al is reduced and the extra electrons may occupy the Al 3s and 3p states to give a localised conducting band. Conversely for O-rich surfaces, electrons may be missing from the O 2p states which characterise the top of the valence band in alumina, and this may provide surface localised conducting states of hole character.

The above picture is consistent with the trends in Mulliken charge documented above, and it is confirmed by calculations of the densities of states on the slabs shown in Fig. 3. These show the empty states at the top of the valence band in O-rich surfaces and the metallic band of electrons in Al-rich surfaces. The strong surface localisation of these surface states is illustrated by the way their charge density decays within two or three atomic layers of the surface. An example is plotted in Fig. 4, which depicts the charge density of a HOMO in the  $\Gamma_{\text{O}} = 1.5$  slab. The stoichiometric surface in these calculations displays a localised state in the gap just below the conduction band, as was found also with the tight-binding model after relaxing the atomic positions.<sup>9</sup>

#### 4.4. Surface energies

The surface energies are plotted as a function of  $p_{\text{O}_2}$  in Fig. 5, using eqn. (7). We see that over almost all the range of pressure up to 1 atmosphere the  $\Gamma_{\text{O}} = 0$  surface has the lowest free energy. Only in UHV could we hope to see the Al-rich surface. This confirms the experimental picture



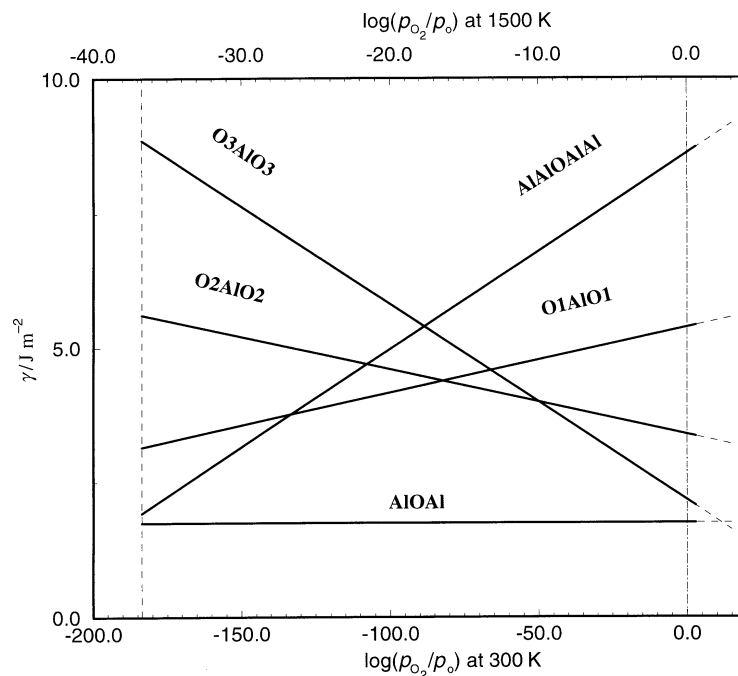


**Fig. 5** Calculated surface energies of various  $1 \times 1$  surfaces as a function of oxygen partial pressure;  $p_0 = 1$  atm. Two different temperatures are shown explicitly by scaling of the horizontal axis according to eqn. (7).

except we have no theoretical data for the observed Al-rich ( $\sqrt{31} \times \sqrt{31}$ )R  $\pm 9^\circ$  surface which has been observed under UHV conditions. It has an oxygen excess  $\Gamma_{\text{O}} = -6$  if the postulated structure<sup>1,2,11,19</sup> is correct, so it would have a very steep slope of surface energy *vs.*  $p_{\text{O}_2}$  on Fig. 5. Depending on the first term in eqn. (7) it may then cut below the  $\Gamma_{\text{O}} = 0$  line on Fig. 5 towards the left of the diagram but at a higher pressure than the  $\Gamma_{\text{O}} = -1.5$  line does. Until the calculations are done this is a matter for speculation.

We certainly expect the O-terminated ( $\Gamma_{\text{O}} = 1.5$ ) surface to be stable at oxygen pressures somewhat greater than 1 atm, but we would not claim sufficient accuracy in our calculations, which neglect the temperature dependence of the first terms in eqn. (7), to make a precise prediction.

## 5. Conclusions

1. We have presented a formalism for calculating the dependence of surface and interfacial energies in oxides on the partial pressure of oxygen, and applied it to compare the energies of five postulated ( $1 \times 1$ ) (0001) surfaces of corundum, differing in their surface stoichiometry. This is essentially a more explicit and somewhat extended version of the formalism used, for example, by Wang *et al.*,<sup>20</sup> who expressed the surface energy in terms of the chemical potential of oxygen. Some subtleties associated with the definition of the zero of energy have been clarified here, and by means of a thermodynamic cycle it has proved unnecessary to calculate any properties of pure oxygen, which would have been problematic.

2. We find that the observed neutral surface, terminated by Al, is stable up to atmospheric pressure. At some higher pressure, perhaps some tens of atmospheres, depending on the temperature, the oxygen-terminated surface would be more stable (see Fig. 5). An Al-rich surface will probably be stable at sufficiently low oxygen pressure, but the most Al-rich surface considered here (two terminating layers) is only theoretically stable at a pressure just below the very low pressure under which corundum would decompose.

3. The relaxed atomic and electronic structures of the surfaces have been obtained. There is qualitative agreement with experimental X-ray diffraction results for the stable surface; this

includes the sign and approximate magnitude of the first four interlayer relaxations, and also the lateral displacements of the surface oxygen atoms, which can be thought of as a rotation and expansion of the oxygen triangle beneath the surface Al. This is explained in terms of electrostatic forces. Ours and previous results both using the local density approximation (or generalised gradient approximation) and Hartree–Fock consistently overestimate the inward relaxation of the surface Al plane compared to the X-ray data. The discrepancy is unresolved. Regarding the second interlayer relaxation, our result (10.6%) is closer to experiment (16%) than previous calculations, some of which omitted lateral relaxations. We have verified, by further tests, that if we do not allow lateral relaxation of oxygen the second interlayer relaxation is suppressed. However, Verdozzi and co-workers<sup>5</sup> using a Gaussian basis, and Wang *et al.*<sup>20</sup> using the full-potential Linear Augmented Plane Wave method have predicted smaller second interlayer relaxations than ours, even though they included lateral relaxations; this requires further investigation, although the discrepancy is less than 0.1 Å.

4. Non-stoichiometric surfaces are metallic. In the case of Al-rich surfaces the Fermi energy lies in a band of surface states below and contiguous with the conduction band. Oxygen-rich surfaces are metallic because of holes at the top of the valence band, which is mainly of O 2p character.

## Acknowledgements

We thank J. Hütter for technical help with the calculations. This work has been supported by the UK Engineering and Physical Sciences Research Council under grants GR/L08380 and GR/M01753. The Centre for Supercomputing in Ireland is gratefully acknowledged for computer resources. This work has benefited from collaborations within, and has been partially funded by, the Training and Mobility Network on “Electronic Structure Calculation of Materials Properties and Processes for Industry and Basic Sciences” (Contract FMRX-CT98-0178).

## References

- 1 G. Renaud, *Surf. Sci. Rep.*, 1998, **32**, 1.
- 2 P. Guénard, G. Renaud, A. Barbier and M. Gautier-Soyer, *Surf. Rev. Lett.*, 1998, **5**, 321.
- 3 I. Manassidis, A. DeVita and M. J. Gillan, *Surf. Sci. Lett.*, 1993, **285**, L517.
- 4 C. Kruse, M. W. Finnis, V. Y. Milman, M. C. Payne, A. DeVita and M. J. Gillan, *J. Am. Ceram. Soc.*, 1994, **77**, 431.
- 5 C. Verdozzi, D. R. Jennison, P. A. Schultz and M. P. Sears, *Phys. Rev. Lett.*, 1999, **82**, 799.
- 6 V. E. Puchin, J. D. Gale, A. L. Shluger, A. A. Kotomin, J. Gunster, M. Brause and V. Kempter, *Surf. Sci.*, 1997, **370**, 190.
- 7 M. Causà, R. Dovesi, C. Pisani and C. Roetti, *Surf. Sci.*, 1987, **215**, 259.
- 8 C. Pisani, M. Causà, R. Dovesi and C. Pisani, *Prog. Surf. Sci.*, 1987, **25**, 119.
- 9 T. J. Godin and J. P. LaFemina, *Phys. Rev. B: Condens. Matter*, 1994, **49**, 7691.
- 10 W. C. Mackrodt, R. J. Davey, S. W. Black and R. Docherty, *J. Cryst. Growth*, 1987, **80**, 441.
- 11 G. Renaud, B. Vilette, I. Vilfan and A. Bourret, *Phys. Rev. Lett.*, 1994, **73**, 1825.
- 12 A. Alavi, J. Kohanoff, M. Parrinello and D. Frenkel, *Phys. Rev. Lett.*, 1994, **73**, 2599.
- 13 A. Alavi, *Philos. Trans. R. Soc. London Ser. A*, 1998, **356**, 263.
- 14 N. Troullier and J.-L. Martins, *Phys. Rev. B: Condens. Matter*, 1991, **43**, 1993.
- 15 I. G. Batyrev, A. Alavi, M. W. Finnis and T. Deutsch, *Phys. Rev. Lett.*, 1999, **82**, 1510.
- 16 I. Mayer, *Chem. Phys. Lett.*, 1983, **97**, 270.
- 17 J. W. Cahn, in *Interfacial Segregation*, ed. W. C. Johnson and J. M. Blakely, American Society for Metals, Metals Park, OH, 1977, pp. 3–23.
- 18 M. W. Finnis, *Phys. Status Solidi A*, 1998, **166**, 397.
- 19 M. Gautier, G. Renaud, L. P. Van, B. Vilette, M. Pollak, N. Thromat, F. Jollet and J.-P. Duraud, *Sci. Alumina*, 1993, **77**, 323.
- 20 X. G. Wang, W. Weiss, S. K. Shaikhutdinov, M. Ritter, M. Petersen, F. Wagner, R. Schlögl and M. Scheffler, *Phys. Rev. Lett.*, 1998, **81**, 1038.

Paper 9/03278I